Metadata of the chapter that will be visualized online

SAND2015-1230C

Chapter Title	Validation of Nonlinear Reduced Order Models with Time Integration Targeted at Nonlinear Normal Modes	
Copyright Year	2015	
Copyright Holder	Springer International Publishing Switzerland	
Author	Family Name	**Kuether**
	Particle	
	Given Name	**Robert J.**
	Suffix	
	Division	Department of Engineering Physics
	Organization	University of Wisconsin
	Address	Madison, WI 53706, USA
	Email	rkuether@wisc.edu
Corresponding Author	Family Name	**Allen**
	Particle	
	Given Name	**Mathew S.**
	Suffix	
	Division	Department of Engineering Physics
	Organization	University of Wisconsin
	Address	Madison, WI 53706, USA
	Email	msallen@engr.wisc.edu
Abstract	Recently, nonlinear reduced order models (ROMs) of large scale finite element models have been used to approximate the nonlinear normal modes (NNMs) of detailed structures with geometric nonlinearity distributed throughout all of its elements. The ROMs provide a low order representation of the full model, and are readily used with numerical continuation algorithms to compute the NNMs of the system. In this work, the NNMs computed from the reduced equations serve as candidate periodic solutions for the full order model. A subset of these are used to define a set of initial conditions and integration periods for the full order model and then the full model is integrated to check the quality of the NNM estimated from the ROM. If the resulting solution is not periodic, then the initial conditions can be iteratively adjusted using a shooting algorithm and a Newton–Raphson approach. These converged solutions give the true NNM of the finite element model, as they satisfy the full order equations, and they can be compared to the ROM predictions to validate the ROM at selected points along the NNM branch. This gives a load-independent metric that may provide confidence in the accuracy of the ROM while avoiding the excessive cost of computing the complete NNM of the full order model. This approach is demonstrated on two models with geometric nonlinearity: a beam with	

clamped-clamped boundary conditions, and a cantilevered plate used to study fatigue and crack propagation.

Keywords (separated by "-")	Reduced order modeling - Geometric nonlinearity - Nonlinear normal modes - Periodic orbits - Finite element analysis

Author's Proof

Chapter 33
Validation of Nonlinear Reduced Order Models with Time Integration Targeted at Nonlinear Normal Modes

Robert J. Kuether and Mathew S. Allen

Abstract Recently, nonlinear reduced order models (ROMs) of large scale finite element models have been used to approximate the nonlinear normal modes (NNMs) of detailed structures with geometric nonlinearity distributed throughout all of its elements. The ROMs provide a low order representation of the full model, and are readily used with numerical continuation algorithms to compute the NNMs of the system. In this work, the NNMs computed from the reduced equations serve as candidate periodic solutions for the full order model. A subset of these are used to define a set of initial conditions and integration periods for the full order model and then the full model is integrated to check the quality of the NNM estimated from the ROM. If the resulting solution is not periodic, then the initial conditions can be iteratively adjusted using a shooting algorithm and a Newton–Raphson approach. These converged solutions give the true NNM of the finite element model, as they satisfy the full order equations, and they can be compared to the ROM predictions to validate the ROM at selected points along the NNM branch. This gives a load-independent metric that may provide confidence in the accuracy of the ROM while avoiding the excessive cost of computing the complete NNM of the full order model. This approach is demonstrated on two models with geometric nonlinearity: a beam with clamped-clamped boundary conditions, and a cantilevered plate used to study fatigue and crack propagation.

Keywords Reduced order modeling • Geometric nonlinearity • Nonlinear normal modes • Periodic orbits • Finite element analysis

33.1 Introduction

Geometric nonlinearity can be encountered in almost any structure where the thickness of a member is small enough that it can deform significantly while the material remains in the linear elastic regime. The development of reduced order models of such systems has been motivated by the efforts of the United States Air Force (USAF) and the National Aeronautics and Space Administration (NASA) to model and design reusable hypersonic aircraft. At hypersonic speeds (Mach > 5) the aerodynamic pressure is sufficient to cause skin panels to vibrate nonlinearly. Additionally, thermal loads can lead to buckling and highly nonlinear vibration of the panel between two buckled states. Similar issues are encountered in stealth aircraft as exhaust from engines, which are buried within the structure to minimize their thermal signature, impinges on structural panels. While these are certainly two extreme environments, it is important to note that geometric nonlinearity can also be encountered in a variety of more common situations. For example, when accelerated endurance tests are performed on structures with thin sheet metal panels, the increased loads may cause the panels, and hence the structure, to behave nonlinearly. This could invalidate the endurance test if the nonlinearity is not considered. As a rule of thumb, a thin panel will tend to behave nonlinearly if the displacement is on the order of the panel thickness, as bending deformations induce axial stretching. This is illustrated schematically in Fig. 33.1 for a clamped-clamped beam.

Finite element codes have been capable of geometrically nonlinear quasi-static analysis for several decades. On today's computers, this type of analysis is feasible for models containing tens or perhaps even hundreds of thousands of degrees of freedom, with solution times on the order of tens of minutes to several hours, respectively. This capability can also be used to compute the transient, dynamic response of the structure, essentially by solving a quasi-static problem at each time step. However, considering the short time steps that are typically required and the time span over which analysis must be performed to obtain meaningful results, a dynamic analysis tends to take thousands if not millions of times longer. Hence,

R.J. Kuether • M.S. Allen (✉)
Department of Engineering Physics, University of Wisconsin, Madison, WI 53706, USA
e-mail: rkuether@wisc.edu; msallen@engr.wisc.edu

© Springer International Publishing Switzerland 2015
G. Kerschen (ed.), *Nonlinear Dynamics, Volume 1*, Conference Proceedings of the Society for Experimental Mechanics Series, DOI 10.1007/978-3-319-15221-9_33

UNCORRECTED PROOF

Author's Proof

this figure will be printed in b/w

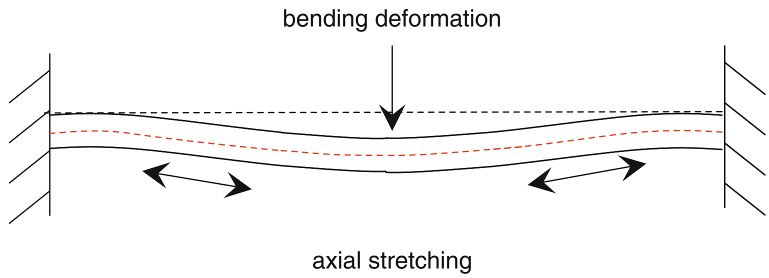

Fig. 33.1 Schematic of clamped-clamped beam subject to bending loads. When the deformations are small axial stretching can be neglected, but for large deformations the total stiffness increases as the beam must both bend and stretch axially to accommodate the deformation

these analyses are far too expensive to be practical as a design tool except perhaps on relatively simple structures or when considering short dynamic events.

Fortunately, in the past few decades Reduced Order Modeling (ROM) approaches have been developed which can extract a lower order dynamic model from a detailed finite element model of a geometrically nonlinear structure and then its response can be computed very inexpensively. The first approach of this kind seems to have been presented by Nash [1], and other early contributors included Segalman and Dohrmann [2, 3], McEwan [4] and Muravyov and Rizzi [5]. All of these methods use a small number of nonlinear quasi-static analyses to extract a low order model for the structure, typically using the structure's linear modal deformation shapes as a basis to describe the nonlinear response. As long as the method used accounts for the way that axial stretching is induced as the structure vibrates in these low order bending modes, an accurate and efficient reduced order model can be obtained. The works by Hollkamp and Gordon [6, 7] provide an excellent review and thorough explanation of the methods. A recent review [8] provides additional perspective on the myriad of methods that have been developed.

While these methods show tremendous promise, it can still be very challenging to create an accurate reduced order model for a real structure. To succeed, not only must one include all of the linear modes that participate in the response, but the static load cases used to determine the ROM must be chosen such that an appropriate level of nonlinearity is excited in each mode's response. If the loads are too small the numerical procedure becomes ill-conditioned and if they are too large they may induce coupling between many modes so that fitting a low order model becomes unacceptable. Furthermore, the number of static load cases required scales with more than the third power of the number of modes (or about the second power for a recent method [9]), so there is strong motivation to use the minimum number of modes that will be adequate.

In order to validate the ROM, most works (see, e.g. [6, 9–12]) have generated responses from either a static or dynamic load applied to the full order finite element model and compared this expensive set of truth data to the response predicted by the ROM. From this truth data, the modes and load levels used to generate the ROM are fine tuned until it agrees acceptably with these results. However, with this approach one cannot assure that the model will suitably agree with the results predicted by the full order model at a different load level, or load type. The authors recently proposed to instead compare the Nonlinear Normal Modes (NNMs) [13–15] of the candidate ROMs and to use them as a metric to gauge the convergence of the ROM [16–18]. Nonlinear modes are typically depicted on a frequency versus amplitude or frequency versus energy plot, which shows how each natural frequency evolves as the response amplitude changes, capturing a more complete amplitude range involving the geometric nonlinearity, independent of any external forces. The NNMs are easy to relate, qualitatively at least, to the response of the structure to sinusoidal [19], transient [17] or even random [20] excitation, so they still provide a powerful connection back to the response to external loads. As a result, the NNMs provide an informative means for comparing two or more candidate ROMs.

This paper builds upon the foundation established in [18], but instead here we discuss in more detail the general procedure that is used to arrive at a valid ROM so that its NNMs agree with the true NNMs of the structure as the number of modes included increases. This paper now proposes to use the deformations found by a ROM to integrate the full model subject to those initial conditions at certain locations along the NNM curve in order to evaluate whether the ROM predicts an NNM solution or not. If the solution is not periodic, than these deformations serve as an initial guess in a shooting algorithm [21] that iterates on the dynamic simulation of the full finite element model over one period until it exhibits a periodic response (to some tolerance) and hence a true NNM. This avoids the lengthy computational effort required to fully resolve the NNM of interest using the continuation algorithm in [21], particularly because one can circumvent the internal resonances where much of the computational effort is expended. These concepts are illustrated on a clamped-clamped beam, one of the simplest structures that exhibits geometric nonlinearity, and on a much more complicated 32,000 DOF model of a specimen used to study the fatigue behavior of Titanium [22].

The paper is outlined as follows. Sect. 33.2 briefly reviews the ROM modeling strategy and the definition of nonlinear normal modes used in this work. The general procedure for generating candidate ROMs and checking the computed NNM solutions on the full order model is also discussed. In Sect. 33.3 the methods are applied to a clamped-clamped beam,

UNCORRECTED PROOF

Author's Proof

capitalizing on the work presented in [18, 21]. The methods are then applied to a fatigue specimen, where the true NNMs are too expensive to compute in detail, providing insight into how these approaches may fare in industrial practice. The conclusions are then presented in Sect. 33.4.

33.2 Theoretical Development

While damping can be included in a ROM [6], the nonlinearity due to large deformations only depends on displacements so this work focuses on the conservative model for the system. After discretization by the finite element method, the system can be represented as,

$$\mathbf{M}\ddot{\mathbf{x}} + \mathbf{K}\mathbf{x} + \mathbf{f}_{NL}(\mathbf{x}) = \mathbf{f}(t) \tag{33.1}$$

where $\mathbf{M}$ and $\mathbf{K}$ are the $N \times N$ linear mass and stiffness matrices and the geometric nonlinearity exerts a nonlinear restoring force through the $N \times 1$ vector, $\mathbf{f}_{NL}(\mathbf{x})$. Note that this nonlinear internal force is purely a static effect. The external loads are accounted for by including the $N \times 1$ vector $\mathbf{f}(t)$, and the $N \times 1$ vectors $\mathbf{x}(t)$ and $\ddot{\mathbf{x}}(t)$ are the displacement and acceleration, respectively.

33.2.1 *Review of Reduced Order Modeling*

A reduced order model is obtained by presuming that the response can be well represented using a small set of mode shapes $\left(\mathbf{K} - {\omega_r}^2\mathbf{M}\right)\boldsymbol{\varphi}_r = 0$ so that,

$$\mathbf{x}(t) = \boldsymbol{\Phi}_m\mathbf{q}(t) \tag{33.2}$$

Each column in the $N \times m$ mode shape matrix, $\boldsymbol{\Phi}_m$, is a mass normalized mode shape vector, φ, and $\mathbf{q}(t)$ is a vector of time-dependent modal displacements. The vectors in $\boldsymbol{\Phi}_m$ are truncated to a small set mode shapes, typically reducing the number of degrees of freedom down to a few tens, or even fewer, of modal coordinates, so $m << N$.

After applying the modal transformation to the full order equations in Eq. 33.1, the equation of motion for each modal degree of freedom becomes

$$\ddot{q}_r + \omega_r^2 q_r + \theta_r\left(q_1, q_2, \ldots, q_m\right) = \boldsymbol{\varphi}_r^{\mathrm{T}}\mathbf{f}(t) \tag{33.3}$$

where ω_r is the linear natural frequency, $()^{\mathrm{T}}$ is the transpose operator and q_r is the r^{th} modal displacement. The nonlinearity couples the modal degrees of freedom so the nonlinear modal restoring force is generally a function of all of the modal displacements $\theta_r(\mathbf{q}) = \boldsymbol{\varphi}_r^{\mathrm{T}}\mathbf{f}_{NL}(\boldsymbol{\Phi}_m\mathbf{q})$. The response of the modes that are excluded from the modal basis is hoped to be negligible. The theory for geometric nonlinearity reveals that the nonlinear modal restoring force can be modeled with second and third order polynomials, which are shown to be

$$\theta_r\left(q_1, q_2, \ldots, q_m\right) = \sum_{i=1}^{m}\sum_{j=i}^{m} B_r(i,j)q_iq_j + \sum_{i=1}^{m}\sum_{j=i}^{m}\sum_{k=j}^{m} A_r(i,j,k)q_iq_jq_k \tag{33.4}$$

The scalars B_r and A_r are the coefficients of the quadratic and cubic nonlinear stiffness terms, respectively, for the r^{th} equation of motion. One approach to determine these coefficients is the Implicit Condensation and Expansion (ICE) method [10], where a series of static loads are applied to the full order model having the shape

$$\mathbf{f} = c_r\mathbf{M}\boldsymbol{\varphi}_r \tag{33.5}$$

with a scaling term c_r defined for the r^{th} mode in the basis set. Note that this force would only cause deformation in a single mode if the system were linear. The *nonlinear* static response of the structure is found in response to the force in Eq. 33.5, and the process is repeated for each mode in the basis and for combinations of up to three modes. With a series of these forces and resulting nonlinear responses, a least squares problem is set up to solve for nonlinear stiffness coefficients B_r and A_r.

UNCORRECTED PROOF

Author's Proof

Another popular ROM approach, termed the Enforced Displacement (ED) method, involves the converse static solutions where a series of modal displacements are applied to the structure and a quasi-static analysis extracts the reaction forces required to hold that displacement [5, 9]. Those forces and displacements are used to solve a series of smaller algebraic equations for the coefficients B_r and A_r. Because a least squares problem is avoided, this method tends to be more numerically stable but it does not implicitly capture the axial effects so axial modes must be included to obtain accurate results.

33.2.2 Review of Nonlinear Normal Modes

The nonlinear normal mode definition used throughout this work is based on the extended definition by Vakakis, Kerschen and others [13, 14], where an NNM is a *not necessarily synchronous periodic solution to the conservative, nonlinear equations of motion*. Each NNM must satisfy the condition of periodicity, and can account for motions that are not synchronous which occur when two or modes interact at a specific integer frequency ratio. Nonlinear modes are typically depicted on a frequency versus energy plot, or FEP, which shows how the natural frequency evolves as the response amplitude changes, revealing many qualitative insights into the amplitude dependent dynamics. Even though the property of superposition and orthogonality no longer hold for the NNM, they are still conceptually useful in the identification of nonlinear dynamics as they form the backbone to the nonlinear forced response curves [13, 14], offer metrics for comparison between nonlinear modeling domains [17, 18, 23–25], and closely follow the freely decaying response of a lightly damped structure as energy dissipates [13, 26].

A pseudo-arclength continuation algorithm, developed originally by Peeters et al. [27], is used throughout this work to compute the NNMs of each of the undamped reduced order models. For the low order m-DOF systems represented by Eqs. 33.3 and 33.4 with $\mathbf{f}(t) = \mathbf{0}$, there exist m nonlinear normal mode branches that each initiate at a linear mode at low energy, or low response amplitude. (Continuation algorithms need an initial solution in order to start tracing an NNM branch, and the linear mode solutions at low energy provide an excellent starting point.) The continuation algorithm uses the shooting technique to find a set of initial conditions and an integration period that satisfy periodicity as the amplitude in the response changes. A shooting function is defined as,

$$\mathbf{H}\left(T, \mathbf{q}_0, \dot{\mathbf{q}}_0\right) = \begin{Bmatrix} \mathbf{q}\left(T, \mathbf{q}_0, \dot{\mathbf{q}}_0\right) \\ \dot{\mathbf{q}}\left(T, \mathbf{q}_0, \dot{\mathbf{q}}_0\right) \end{Bmatrix} - \begin{Bmatrix} \mathbf{q}_0 \\ \dot{\mathbf{q}}_0 \end{Bmatrix} = \{\mathbf{0}\}, \tag{33.6}$$

where T is the period of integration, and $\mathbf{q}_0$ and $\dot{\mathbf{q}}_0$ are the initial modal displacements and velocities, respectively, for a candidate ROM. The ROM equations must be integrated over a period T subject to the initial conditions $\mathbf{q}_0$ and $\dot{\mathbf{q}}_0$ to evaluate whether or not these variables produce an NNM motion. The periodicity condition is based on a numerical tolerance $\varepsilon_{\text{shoot}}$, such that an NNM motion is obtained when

$$\frac{\left\|\mathbf{H}\left(T, \mathbf{q}_0, \dot{\mathbf{q}}_0\right)\right\|}{\left\|\begin{Bmatrix} \mathbf{q}_0 \\ \dot{\mathbf{q}}_0 \end{Bmatrix}\right\|} < \varepsilon_{\text{shoot}} \tag{33.7}$$

Typically a numerical tolerance $\varepsilon_{\text{shoot}}$ on the order of 10^{-4} to 10^{-6} is used, depending on the accuracy of the numerical time integration scheme. Once periodicity is satisfied, an NNM solution is uniquely defined by $\mathbf{q}_0$, $\dot{\mathbf{q}}_0$, and T, which is used with the continuation algorithm to predict a new periodic solution at a slightly different energy level. A step size controller determines the magnitude of the prediction step based on the number of iterations taken during the preceding correction steps.

33.2.3 Proposed Procedure for Generating a Valid ROM

The authors have developed the following procedure to obtain a valid ROM for a finite element model of interest using its computed NNMs as a convergence metric, as originally proposed in [18]. The analyst must first select the frequency and energy range of interest, and ultimately choose which nonlinear normal modes it should accurately compute. In this section, the procedure is outlined for a ROM that will only capture the NNM that initiates from the r^{th} mode of interest. Note that the procedure is similar for a ROM that needs to accurately compute many different NNMs.

UNCORRECTED PROOF

Author's Proof

1. For a given force amplitude c_r in Eq. 33.5, compute both the linear and nonlinear static response for the r^{th} mode of interest. As an initial guess, determine the load scaling c_r that would give one thickness of deformation for the linear response.
   (a) If the ratio of the nonlinear displacement to the linear displacement is not between about 0.85 and 0.90, or 1.15 and 1.10, repeat with a larger or smaller load. This general rule of thumb has been found [6, 18] to activate the nonlinearity sufficiently so that B_r and A_r can be accurately determined from the static load cases.
2. Use $\mathbf{q} = \mathbf{\Phi}^{T}\mathbf{Mx}$ to compute the modal displacement of each mode in response to the load case in step (1). Identify any modes that are strongly coupled (statically) to the mode of interest.
3. Compute a 1-Mode ROM using only the r^{th} mode and compute the NNM from those equations.
4. Add a few of the modes that were most strongly coupled to the r^{th} mode in step (2). For the added modes, determine the appropriate scale levels, and compute a multi-mode ROM with the new mode set.
5. Recompute the NNM using the improved multi-mode ROM of interest. Compare the NNM with that found in step (3).
6. If the NNM has not converged, one can either:
   (a) Repeat the analysis in steps (4) through (5) by adding any additional modes to the ROM identified from step (2) and using the appropriate load levels.
   (b) Consider whether smaller or larger load levels should be used when generating the multi-mode ROM and repeat steps (4) through (5).

In the authors' previous work, the convergence of the ROM was evaluated based on the NNMs, just as outlined above, but these results were ultimately deemed accurate by comparing those to the NNM computed directly from the full finite element model using the Applied Modal Force (AMF) continuation algorithm in [21]. The AMF results are costly for large scale models since the continuation algorithm uses many time integrations of the full model to iterate on the initial conditions to satisfy the shooting function at many point along the NNM branch. The authors also found that much computational effort was wasted seeking to map out the NNM branch through internal resonances where several modes respond and the frequency-energy behavior is complicated, hence requiring many prediction/correction steps. This work approaches the final validation step a little differently. Instead of running AMF on the full model to get the truth data, the NNM computed from the ROMs using the procedure above is checked at a few points on the curve by integrating the full model subject to the initial conditions found using the ROMs, thus requiring fewer numerical simulations on the full model.

Specifically, suppose that one ROM denoted ROM_A, involving a certain set of modal coordinates $\mathbf{q}_{ROM}$ (for example, the result for the ICE (1,3,5,7) ROM in Sect. 33.3.1 includes q_1, q_3, q_5 and q_7) produces a periodic response at a certain point along the frequency energy curve with initial conditions $\mathbf{q}_{ROM,0}$, $\dot{\mathbf{q}}_{ROM,0}$ and integration period T. These initial conditions are then used to compute the initial bending displacement at each point in the FE model using

$$\mathbf{x}_{b,0} = \mathbf{\Phi}_{ROM}\mathbf{q}_{ROM,0} \tag{33.8}$$

and similarly for the velocities. Then the expansion procedure in ICE [10] is used to compute the corresponding membrane deformations $\mathbf{x}_{m,0}$ and the two are added $\mathbf{x}_{tot,0} = \mathbf{x}_{b,0} + \mathbf{x}_{m,0}$ to estimate the total deformation of the structure corresponding to the point of interest. The result is then used as the initial condition for the full FE model. Note that when the enforced displacements procedure is used the membrane modes are explicitly included in the ROM so Eq. 33.8 produces the total deformation $\mathbf{x}_{tot,0}$ directly.

The finite element model is integrated subject to these initial conditions and the response after one cycle is extracted. This is then used to check the quality of the solution for the NNM at this point by computing the shooting function (in terms of the displacements only) as,

$$\mathbf{H}\left(T, \mathbf{x}_{tot,0}, \dot{\mathbf{x}}_{tot,0}\right) = \mathbf{x}\left(T, \mathbf{x}_{tot,0}, \dot{\mathbf{x}}_{tot,0}\right) - \mathbf{x}_{tot,0} \tag{33.9}$$

The convergence metric is similar to the one in Eq. 33.7, such that

$$\frac{\left\|\mathbf{H}\left(T, \mathbf{x}_{tot,0}, \dot{\mathbf{x}}_{tot,0}\right)\right\|}{\left\|\mathbf{x}_{tot,0}\right\|} = \varepsilon \tag{33.10}$$

In previous works [21] the authors used a tolerance threshold of 10^{-4} to realize a periodic solution within a finite element code. This procedure is repeated at a few key points of interest on the NNM and used to assess how well the ROM represents the full finite element model.

UNCORRECTED PROOF

Author's Proof

If the candidate initial conditions do not provide an adequate periodic solution, then the Newton–Raphson approach can be used to iterate on the initial conditions supplied by the ROM until the shooting function is satisfied to a preferred numerical tolerance. This is the same approach used in the shooting portion of the AMF algorithm in [18] with the initial conditions determined as follows. First, a nonlinear static analysis is performed to compute the reaction forces, $\mathbf{f}_{\mathrm{tot},0}$, required to hold the structure at the displacement $\mathbf{x}_{\mathrm{tot},0}$ estimated from the ROM. Then, those reaction forces are projected onto each of the modes in the ROM basis as,

$$\widehat{\mathbf{f}}_{tot,0} = \mathbf{\Phi}_{\mathrm{ROM}}{}^{\mathrm{T}}\mathbf{f}_{\mathrm{tot},0} \tag{33.11}$$

where $\widehat{\mathbf{f}}_{\mathrm{tot},0}$ is the $m \times 1$ vector of modal force amplitudes. The initial conditions $\mathbf{x}_{\mathrm{FE},0}$ used to evaluate the shooting function in Eq. 33.9 are then determined by solving the nonlinear static response of the full model to the force $\mathbf{M\Phi}_{\mathrm{ROM}}\widehat{\mathbf{f}}_{\mathrm{tot},0}$. The full finite element model is integrated to these initial conditions to check for periodicity, and the free variables $\widehat{\mathbf{f}}_{\mathrm{tot},0}$ and T are updated using a Newton–Raphson approach until the shooting function is satisfied. Additional modal forces can be added if convergence is not obtained, as outlined in [21]

33.3 Numerical Results

The proposed approach was applied to two different geometrically nonlinear finite element models: a clamped-clamped beam that was modeled with forty B31 beam elements, and a flat cantilevered plate with over 30,000 degrees of freedom. Both models were created and evaluated in Abaqus®, although in other works Nastran® [9] and Ansys® [16] have also been shown to have similar capabilities.

33.3.1 Clamped-Clamped Beam from [18, 21]

The ROMs of the clamped-clamped beam and the approach used to find them were described thoroughly in [16, 18], so only the final result will be highlighted here and used to explore whether the metric in Eqs. 33.9 and 33.10 can be effectively used to discern between candidate ROMs. In [18], a 1-mode ROM denoted ICE (1) (e.g. a ROM generated with Implicit Condensation and Expansion with only mode 1 in the basis) was found to accurately capture the backbone of the beam's first NNM, and a ROM that included modes 1, 3, 5 and 7, denoted ICE (1,3,5,7), captured the backbone more accurately and also two of its modal interactions. An ED (1) ROM will also be considered here, as an example of a ROM that does not as accurately reflect the structure. Recall that axial modes must be included in the Enforced Displacement method to obtain an accurate ROM. In [18] the authors show that an ED (1,26,39) ROM can be created that has similar accuracy to the ICE (1) ROM. The frequency energy plot (FEP) of the first NNM computed from each of these models is shown in Fig. 33.2a.

One can see that the FEPs predicted by the ICE (1) and ICE (1,3,5,7) ROMs agree very well with each other, except for the fact that the former misses the 5:1 modal interaction with NNM 3 at 88 Hz. Because these successive ROMs agree along the backbone, one might expect that they correspond to the true NNM, but in practice it can sometimes be difficult to be sure that convergence has been achieved. For example, it is possible that a ROM with additional degrees of freedom, for example an ICE (1,3,5,7,9,11) ROM, will encounter numerical ill conditioning and give a different answer. As a first attempt to evaluate the quality of these ROMs, four points were selected (as shown with markers in Fig. 33.2a) and the full model was integrated over one cycle with the initial conditions corresponding to those of the ROM at each of these points. The shooting tolerance was then computed using Eq. 33.10 and the result is shown in Fig. 33.2b. The most refined ROM gave a tolerance near 0.001, indicating that the full finite element model very nearly satisfies the shooting function for the initial conditions that the ROM supplies. For reference, the authors used a tolerance of 0.0001 in the AMF algorithm described in [21] to compute the "true" NNMs of this structure. Similarly, the results show that the ICE (1) ROM is quite adequate in some cases while one can expect errors of $0.1 < \varepsilon < 0.5$ if the ED (1) ROM is used.

Certainly this evaluation of four points is not nearly as robust as the comparisons that were used in [18], where the NNMs from each ROM were compared with the NNMs computed from the full FEA model. However, it only took about 30 s per point to evaluate the shooting function in Eq. 33.9, while the AMF algorithm would take about two hours to compute the backbone of this NNM over the same range, and even more time for the internal resonances. On larger systems this difference will be even more dramatic. The time histories of the nodal transverse displacements are shown in Fig. 33.3 for the solutions near 115 Hz in Fig. 33.2a, revealing the degree to which the displacements differ from a true, periodic response (and hence

UNCORRECTED PROOF

Author's Proof

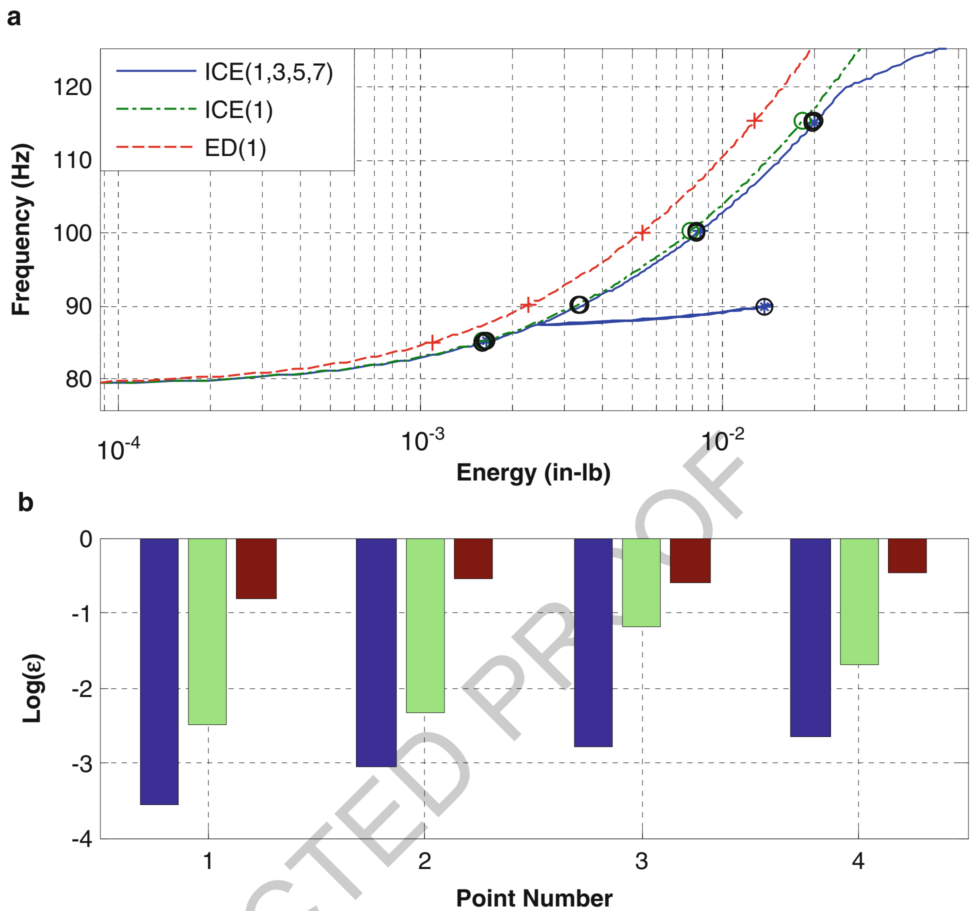

Fig. 33.2 (**a**) Frequency-energy plot showing the first NNM of various ROMs, and (*black circles*) represent converged NNMs with the full FE model. (**b**) Base 10 logarithm of the shooting tolerance, ε, in Eq. 33.10

this figure will be printed in b/w

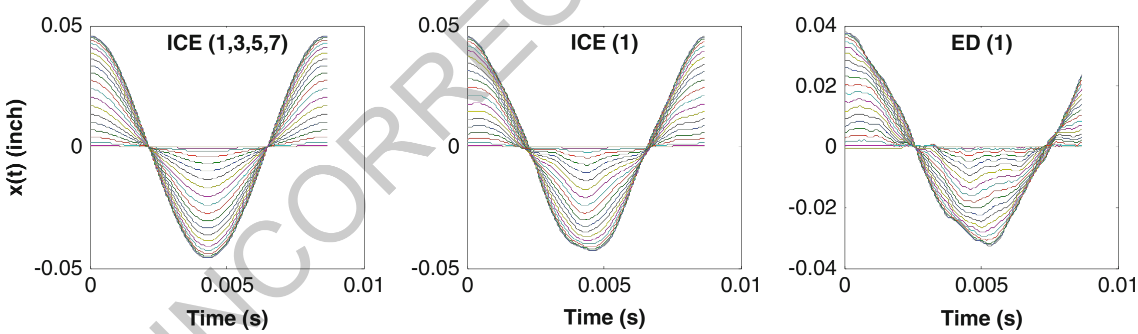

this figure will be printed in b/w

Fig. 33.3 Time histories found after integrating the full FEA model subject to the initial conditions prescribed by each of the ROMs for the points near 115 Hz in the FEP in Fig. 33.2

UNCORRECTED PROOF

an NNM). The response from the ICE (1,3,5,7) ROM initial conditions appears to be periodic, whereas the ED (1) ROM clearly does not predict the correct initial conditions to satisfy the full model. One could similarly compute the time history of a different quantity of interest, such as strain or stress, to determine whether its deviation from perfect periodic motion is large enough to invalidate life predictions or other key quantities of interest.

To further evaluate the quality of the ROMs, the black circles shown in Fig. 33.2a are converged NNM solutions using the shooting algorithm to drive the tolerance below 0.0001, as done in the AMF algorithm. The initial conditions were seeded from each of the ROMs at the four points of interest. During the Newton–Raphson iteration, the period of integration was held fixed, therefore the algorithm only converged on solutions with the same initial frequency. Therefore, the percent errors in the ROM energy and true energy, as shown in Table 33.1, can be used to gauge how close the ROM is to the truth model. For each of the points on the ICE (1,3,5,7), the shooting algorithm took at most two iterations (approximately 7 min) to converge below a tolerance of $\varepsilon < 0.0001$. The algorithm converged in anywhere between two to four iterations with the

Author's Proof

Table 33.1 Percent error of energy after AMF shooting converged to true NNM solution

Point	Energy error ED (1)	Energy error ICE (1)	Energy error ICE (1,3,5,7)
1	56.4 %	8.4 %	1.8 %
2	51.2 %	4.8 %	1.8 %
3	47.8 %	2.4 %	0.1 %
4	46.0 %	1.3 %	0.1 %

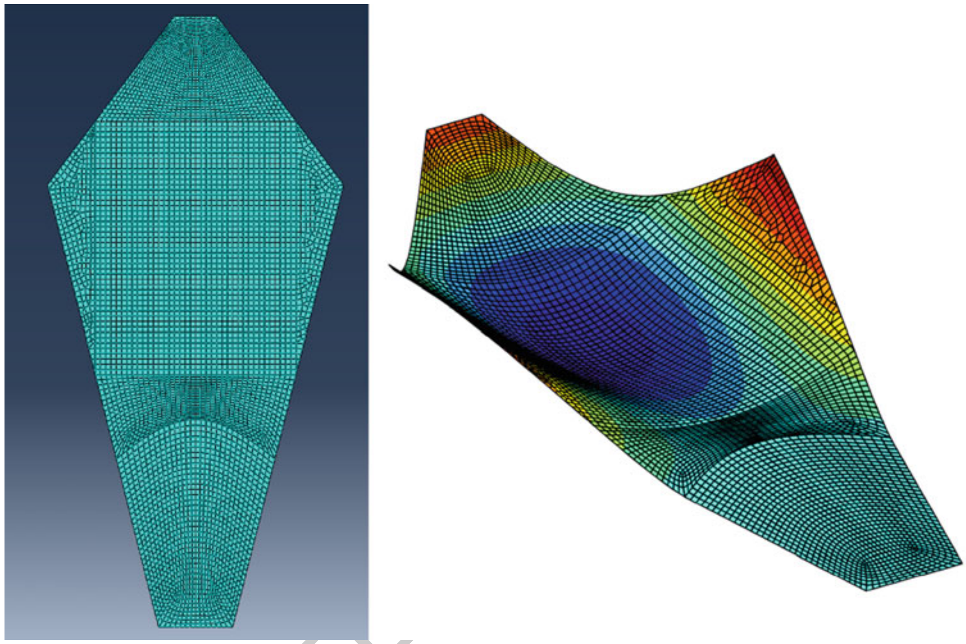

Fig. 33.4 (*left*) Finite element model used to model the cantilevered flat plate (*right*) 7th bending mode

this figure will be printed in b/w

ICE (1) NNM as starting guesses, and between three to five for the ED (1) NNM. The results suggests that if fewer than about 15 points on the NNM were desired then it would be cheaper (for this system) to compute the ROM first and then use its NNM to seed the shooting algorithm at each desired point.

The NNMs predicted by the ICE (1,3,5,7) ROM match the energy, within 2 % error, of that predicted by the NNM of the full model at 4 frequency locations along the NNM: three points along the backbone and one along the tongue of the 5:1 internal resonance with NNM 3. Also, the initial conditions predicted by the ICE (1,3,5,7) ROM reasonably satisfies the periodicity condition from the full FE model at the same four points. Both of these observations suggest that one can have confidence that the other solutions along the backbone are also accurate, and that the ROM has converged to solutions on NNM 1. The fact that the NNM has converged has important implications. For example, if the structure is lightly damped, then one can show [19], that the forced response of the ROM (in the worst case resonant condition) is also likely to agree over this same range of energy.

UNCORRECTED

33.3.2 Cantilevered Plate

The next system studied is a cantilevered plate used to test the fatigue strength of materials and to validate models that simulate crack growth [28]. The shape of the plate and sinusoidal clamp at the bottom edge cause this plate to have a two-stripe mode (mode with two vertical node lines) where the region of highest stress is in the center of the top portion of the plate. The design was optimized to minimize the stresses near the clamp because it is difficult to control the stress field and to limit crack initiation in that region. The plate was modeled with a total of 5,378 nodes using a mixture of S3 and S4 shell elements, as shown in Fig. 33.4. The material properties of the model are those of a titanium alloy, having a Young's Modulus of 17.92 Mpsi, density of 0.164 lb/in^3, and a Poisson's ratio of 0.291. The thickness of the plate was 0.0511 in. Springs are connected to each node below the curve in the out of plane direction. The bottom edge of the plate is constrained in the vertical direction and the bottom-left node is constrained in the horizontal direction. The model was updated based on experimental data to determine the stiffness of the springs (k = 141 lb/in for the model used in this work), and a comparison of the linear natural frequencies of the plate are shown below in Table 33.2.

Author's Proof

Table 33.2 Linear natural frequencies of the cantilevered plate

Mode number	Experimental Nat. Freq. (Hz)	FE Nat. Freq. (Hz)
1	27.7	28.424
2	98.6	99.501
3	167.9	169.71
4	437.6	436.95
5	566.0	567.65
6	756.9	754.03
7	861.1	848.07
8	1,041.3	1,048.6
9	1,206.5	1,188.8
10	1,378.5	1,370.6
11	1,408.4	1,396.4
12	1,608.9	1,607.5
13	2,043.3	1,983.6
14	2,062.8	2,066.3

UNCORRECTED PROOF

The key mode of interest of this plate is the two stripe mode, Mode 7, which is the only mode that is significantly excited during fatigue testing. During the endurance test, the plate is excited with a base excitation at a monoharmonic frequency near Mode 7's natural frequency and typically at a large enough response amplitude to cause the plate to exhibit significant geometric nonlinearity. As a result, it is important to capture the 7th NNM when creating a ROM that will be used to model the response to such harmonic excitation. O'Hara and Hollkamp have successfully predicted both the direction and the rate of crack growth using a reduced order model in combination with the generalized finite element method (GFEM) [28]. When selecting a modal basis for the ROM, one should include any modes that are nonlinearly coupled with linear Mode 7, as these will influence the deformation field, and hence stress distribution, that will drive crack growth.

As a result, Mode 7 was used to seed the process presented in Sect. 33.2.3 and various load scales were applied using Eq. 33.5 to evaluate its nonlinearity and the modes statically coupled to it. The result is shown below in Fig. 33.5, where the vertical axis shows the modal displacement amplitude, and the horizontal axis shows the maximum linear displacement to thickness ratio if the force in the shape of Mode 7 were applied to the linear structure. A force-displacement analysis with 60 static solutions takes about 17 min for this model. This analysis revealed that the displacement must reach between 2 and 4 plate thicknesses to see appreciable nonlinearity. The results of these loadings were also used to determine which linear modes of the structure were activated and hence statically coupled to Mode 7. As shown in Fig. 33.5, Modes 1, 3 and 6 are most strongly coupled (statically) to Mode 7, so they were the next candidates to add to the model.

On the first iteration, a one mode ROM was created with a force that would have displaced Mode 7 two times the thickness, denoted ICE (7) CD (2). Based on the couplings observed above, a 4-mode ROM was then created and additional static load cases were performed for Mode 1 and 3 and linear displacements CD (10,3,1,2) were determined to be suitable (the values for Modes 1 and 3 were determined through additional force-displacement calculations, while that for Mode 6 was assumed to avoid computing an additional set of static load cases). These displacements caused nonlinear displacements that, respectively, had the following ratios relative to the computed linear displacement: 0.995, 0.84965, 0.6174, 1.1476. The first value is well outside the desired range of 0.85–0.9, but little nonlinearity was expected from this fundamental cantilever mode. It was hoped that this load level would be adequate to assure that the ROM did not prematurely predict nonlinear response in this mode, while being small enough to avoid contaminating the other modes. For reference a second ROM was created with the same modes and using CD (1,1,1,1), which could be considered an approach based on blindly applying a rule of thumb. Finally, an even higher order ICE (1,3,6,7,9,10,12) ROM was generated with the load case CD(10,3,1,2,1,1,1), referred to as Case 1. Case 2 was also generated with the same modes, but instead using half as large of force amplitudes when creating the ROM.

Figure 33.6 shows the NNM for Mode 7 computed with each of these ROMs. The NNM computation has revealed that there are quite significant differences between the five ROMs and the variations are such that it is difficult to say which of these ROMs might be most accurate. One might wonder, which load cases will give the best results? Will adding modes increase the accuracy due to the more complete modal basis, or decrease it as numerical ill conditioning becomes more severe?

Three points were identified on the NNM computed with each of the ROMs, as shown with black squares in Fig. 33.6, and were used to initiate a transient response on the full finite element model. About 42 min were required to compute each of the nonlinear transients and to write the response (at all nodes) to disk at all time instants during the response. The resulting shooting tolerances in Eq. 33.10 are summarized in Table 33.3, suggesting that both of the seven mode ROMs are similar

Author's Proof

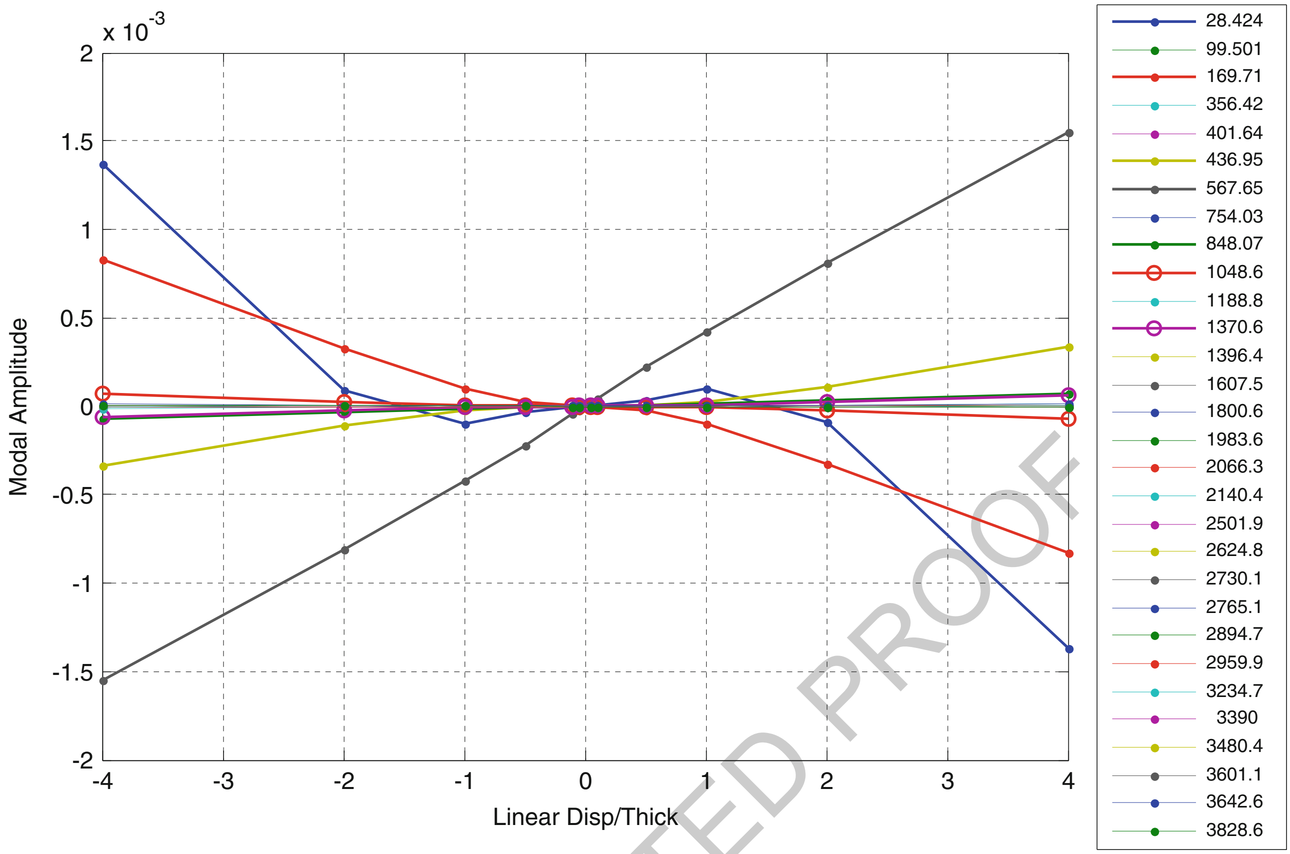

this figure will be printed in b/w

Fig. 33.5 Force-displacement analysis of the plate when a force in the shape of Mode 7 is applied to the nonlinear finite element model. The *colored lines* represent the modal amplitudes of the statically coupled modes, whose linear natural frequencies are in the legend

UNCORRECTED PROOF

and quite close to the true NNM of the FEA model at the first two points. At the higher energy level, these ROMs apparently deviate quite a bit from the true NNM, so the ROM may need to be further refined if that regime is of interest. At point 1 the ICE (1,3,6,7) ROMs agree fairly closely with the higher order ROMs, so either of these might be close to the true NNM as well, explaining why the FEPs of all the multi-mode ROMs nearly agree around 580 Hz in Fig. 33.6.

In order to illustrate how these values of ε relate to the error in the solution, the time history of modal displacements over the integration period is shown for points 1, 2 and 3 using the ICE (1, 3, 6, 7, 9, 10, 12) CD (10, 3, 1, 2, 1, 1, 1) ROM. The physical displacements from the full finite element model were projected onto the unit displacement normalized modes, such that the modal degrees of freedom have units of inches. Each of these time histories are plotted below in Fig. 33.7, showing just the first 8 most dominant modes of each response from the full order model.

The integrated response from points 1 and 2 show that the solution is nearly periodic, although point 2 begins to have significant contributions from the other modes coupled to Mode 7. The significant error in ε for the response at point 3 may be attributed to the fact that modes 14, 16 and 18 become excited, indicating that these modes are dynamically coupled to Mode 7 and may need to be included in the ROM to more accurately compute NNM 7. It is interesting that there is noticeable difference in modal amplitude of Mode 7 from $t = 0$ to the final time. This suggests that this mode is not well represented in the ROM or that coupling with other modes has caused it to deviate from a periodic response. The time histories show how ε reveals the inaccuracy of the ROM at point 3, however the response at points 1 and 2 would be considered acceptable.

Based on these results, the next step would be to generate a ROM with additional modes (14, 16 and 18) and track how the NNM computed from the new ROM compares to the ones in Fig. 33.6. The initial conditions from these NNMs could then be used to seed the shooting algorithm discussed in Sect. 33.2.3, providing further insight into the location of the true NNM of the full order model and whether any of the ROMs capture these solutions. Neither of these items were explored in this work, but will certainly be considered in the future. Also, so far only NNM 7 has been studied in detail, but in reality it is significantly affected by the other NNMs that are extensions of the linear modes in the basis. Modal interactions with NNM 7 are strongly dependent on the accuracy of the other NNMs generated by the ROM, therefore it would probably be wise to assess the convergence of those NNMs.

Author's Proof

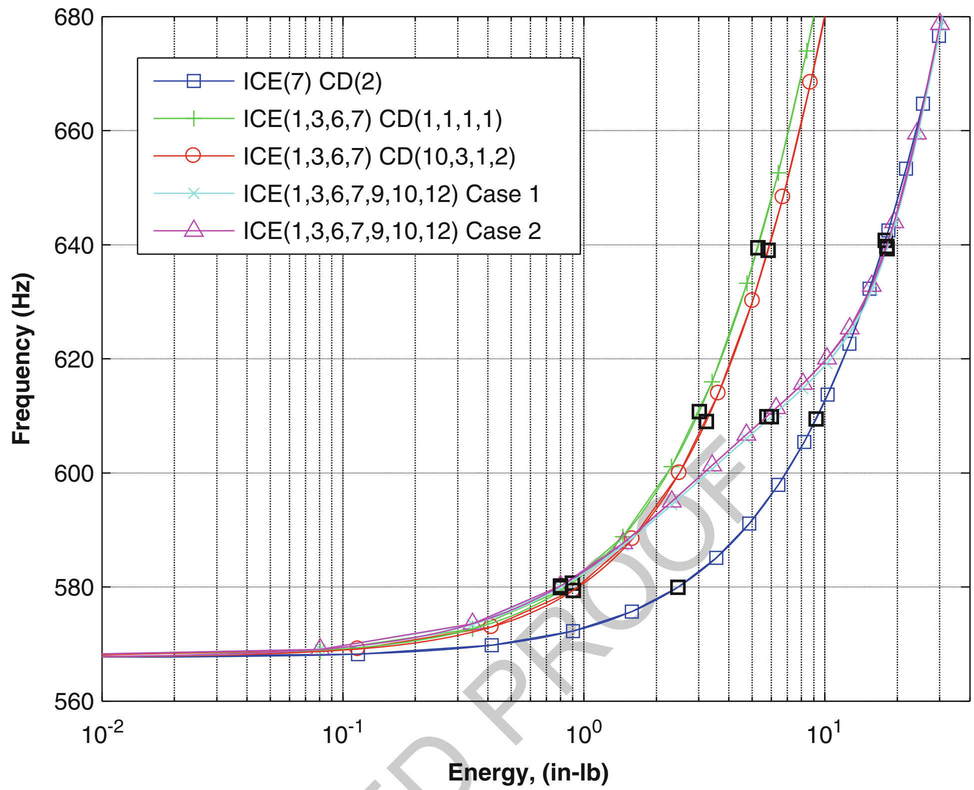

Fig. 33.6 Estimate of 7th NNM computed from various ROMs of the cantilevered plate. In the last two lines of the legend, Case 1 corresponds to CD(10,3,1,2,1,1,1) while Case 2 used forces half as large with CD(5,1.5,0.5,1, 0.5, 0.5, 0.5)

this figure will be printed in b/w

UNCORRECTED PROOF

Table 33.3 Values of shooting function tolerance, ε, from Eq. 33.10 for the points shown with black squares in Fig. 33.6

Point	Frequency (Hz)	ε ICE (7) CD (2)	ε ICE (1,3,6,7) CD (1,1,1,1)	ε ICE (1,3,6,7) CD (10,3,1,2)	ε ICE (1,3,6,7,9,10,12) CD (10,3,1,2,1,1,1)	ε ICE (1,3,6,7,9,10,12) CD (5,1.5,0.5,1,0.5,0.5,0.5)
1	580	0.241	0.0853	0.0875	0.00896	0.00897
2	610	0.344	0.205	0.216	0.0663	0.0657
3	640	0.396	0.267	0.278	0.177	0.173

33.4 Conclusion

This work explores a systematic approach to obtain validated reduced order models from finite element models with geometric nonlinearity based on their computed nonlinear normal modes. Ideally, as more modes are added to the basis set, or the scaling of the loads are adjusted, these low order equations should converge and accurately predict the NNMs of the full order model. In this paper, the ROMs provide a set of initial conditions from the predicted NNM, which are integrated with the full order model to check the quality of the ROM. A small set of points along the branch can be selected to span the desired range of response amplitude, covering a more complete operating range of interest. If the initial conditions of the ROMs do not produce periodic motions, they can be iteratively adjusted using the shooting algorithm and a Newton–Raphson approach in hopes of converging on a true NNM. These converged solutions provide further insight into the deficiencies of the ROM. This approach avoids the need to run the costly AMF continuation algorithm [21] to trace the full NNM branch directly from the full finite element model, which has shown to require many more time integrations, and has a tendency to waste a lot of computational effort when tracing out the internal resonances.

The approach was demonstrated on a simple beam with geometric nonlinearity and fixed boundary conditions at both ends. The ICE ROM had nearly converged on the backbone of the 1st NNM using only a single-mode ROM, and captured one of the beams internal resonances when using four modes. The initial conditions supplied by these ROMs were integrated with the full finite element model and produced acceptable NNMs. Even the converged NNMs found with the shooting algorithm agreed very well with these ROMs, validating them at various energies and frequencies. The single-mode ED

Author's Proof

this figure will be printed in b/w

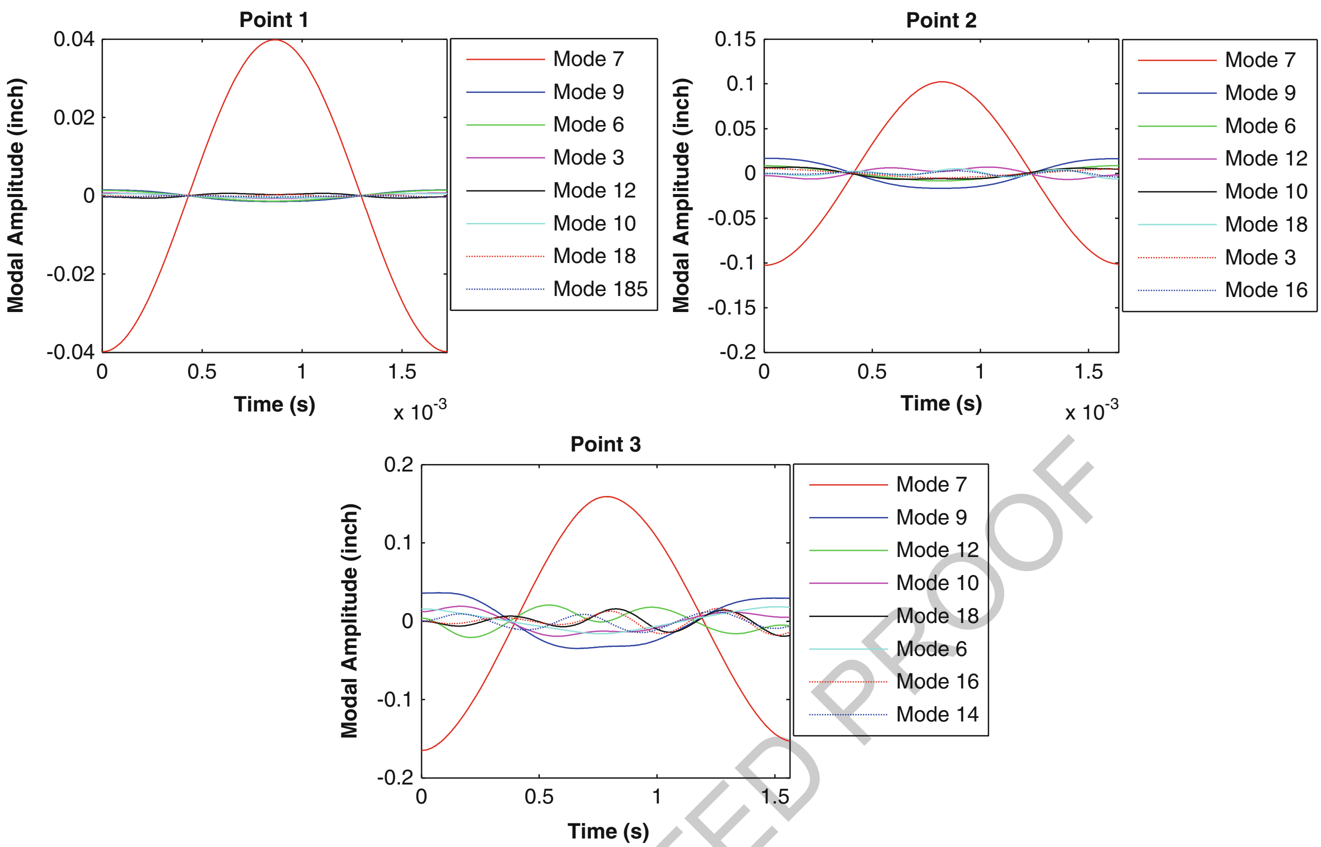

Fig. 33.7 Time histories of the integrated response of the full order model for the points shown with *black squares* in Fig. 33.6 using the ICE (1, 3, 6, 7, 9, 10, 12) CD (10, 3, 1, 2, 1, 1, 1) ROM. The first eight most dominant modal displacements are shown over one integration period

ROM did not perform as well (as predicted due to the lack of membrane modes in the basis) since the estimated backbone was much stiffer than the true NNM, resulting in integrated responses that were clearly not periodic and FEPs that were far of from the true NNM. A cantilever plate model with 32,000 degrees of freedom was used as an industrial application where this approach might be useful. The ICE ROMs with various mode shapes showed that the 7th NNM of interest was difficult to accurately capture, as no convergence was observed in the FEPs. Integrating the initial conditions at three points along the branch with each ROM revealed that the ROMs may be converging at lower energies, but more deformation shapes would be needed in the ROM basis to capture the higher energy response. The results revealed that as more modes were added to the basis, the evaluation of the shooting function improved, suggesting that the ROMs were converging to the true solution.

This procedure shows great promise as an approach to validate a ROM without having to run very many overly expensive time simulations on the full order model. One can choose the operating range of interest for the ROM, and validate it at those energy levels, or frequencies. The NNM is independent of any external forces applied to the structure, providing a more robust comparison metric between candidate ROMs and the full order model. In future works, additional modes will be added to the ICE ROM of the cantilever plate in hopes of further improving the prediction of the 7th NNM. Also, the shooting algorithm will be used to find true NNMs at select points along the backbone, in hopes of guiding further improvements to the ROM procedure, or validating the existing ones. Other NNMs will be considered as well.

Acknowledgements The authors gratefully acknowledge the support of the Air Force Office of Scientific Research under grant number FA9550-11-1-0035, administered by the Dr. David Stargel of the Multi-Scale Structural Mechanics and Prognosis Program. The authors also wish to thank Dr. Joseph Hollkamp and the Structural Sciences Center at the Air Force Research Laboratory for providing the Abaqus® interface that was used in this work as well as for many helpful suggestions and discussions regarding the ROM modeling.

UNCORRECTED PROOF

Author's Proof

References

1. Nash M (1977) Nonlinear structural dynamics by finite element modal synthesis. PhD, Department of Aeronautics, Imperial College
2. Segalman DJ, Dohrmann CR (1996) Method for calculating the dynamics of rotating flexible structures, Part 1: derivation. J Vib Acoust Trans ASME 118:313–317
3. Segalman DJ, Dohrmann CR, Slavin AM (1996) Method for calculating the dynamics of rotating flexible structures, Part 2: example calculations. J Vib Acoust Trans ASME 118:318–322
4. McEwan MI, Wright JR, Cooper JE, Leung AYT (2001) A combined modal/finite element analysis technique for the dynamic response of a non-linear beam to harmonic excitation. J Sound Vib 243:601–624
5. Muravyov AA, Rizzi SA (2003) Determination of nonlinear stiffness with application to random vibration of geometrically nonlinear structures. Comput Struct 81:1513–1523
6. Gordon RW, Hollkamp JJ (2011) Reduced-order models for acoustic response prediction. AFRL-RB-WP-TR-2011-3040, July 2011
7. Hollkamp JJ, Gordon RW, Spottswood SM (2005) Nonlinear modal models for sonic fatigue response prediction: a comparison of methods. J Sound Vib 284:1145–1163
8. Mignolet MP, Przekop A, Rizzi SA, Spottswood SM (2013) A review of indirect/non-intrusive reduced order modeling of nonlinear geometric structures. J Sound Vib 332:2437–2460
9. AQ1 Perez R, Wang XQ, Mignolet MP (2014) Nonintrusive structural dynamic reduced order modeling for large deformations: enhancements for complex structures. J Comput Nonlin Dyn 9:031008
10. Hollkamp JJ, Gordon RW (2008) Reduced-order models for nonlinear response prediction: implicit condensation and expansion. J Sound Vib 318:1139–1153
11. Przekop A, Guo X, Rizzi SA (2012) Alternative modal basis selection procedures for reduced-order nonlinear random response simulation. J Sound Vib 331:4005–4024
12. Rizzi SA, Przekop A (2008) System identification-guided basis selection for reduced-order nonlinear response analysis. J Sound Vib 315:467–485
13. Kerschen G, Peeters M, Golinval JC, Vakakis AF (2009) Nonlinear normal modes. Part I. A useful framework for the structural dynamicist. Mech Syst Signal Process 23:170–194
14. Vakakis AF (1997) Non-linear normal modes (NNMs) and their applications in vibration theory: an overview. Mech Syst Signal Process 11:3–22
15. AQ2 Vakakis AF, Manevitch LI, Mikhlin YN, Pilipchuk VN, Zevin AA (1996) Normal modes and localization in nonlinear systems. Wiley, New York
16. Allen MS, Kuether RJ, Deaner BJ, Sracic MW (2012) A numerical continuation method to compute nonlinear normal modes using modal coordinates. In: 53rd AIAA/ASME/ASCE/AHS/ASC structures, structural dynamics, and materials conference, Honolulu
17. Kuether RJ, Brake MR, Allen MS (2014) Evaluating convergence of reduced order models using nonlinear normal modes. Presented at the 32nd international modal analysis conference (IMAC XXXII), Orlando
18. AQ3 Kuether RJ, Deaner BJ, Hollkamp JJ, Allen MS (2014) Evaluation of geometrically nonlinear reduced order models with nonlinear normal modes. AIAA J (submitted)
19. Peeters M, Kerschen G, Golinval JC (2011) Dynamic testing of nonlinear vibrating structures using nonlinear normal modes. J Sound Vib 330:486–509
20. Schoneman JD, Allen MS, Kuether RJ (2014) Relationships between nonlinear normal modes and response to random inputs. Presented at the 5th AIAA/ASME/ASCE/AHS/SC structures, structural dynamics, and materials conference, National Harbor
21. Kuether RJ, Allen MS (2014) A numerical approach to directly compute nonlinear normal modes of geometrically nonlinear finite element models. Mech Syst Signal Process 46:1–15
22. O'Hara PJ, Hollkamp JJ (2014) Modeling vibratory damage with reduced-order models and the generalized finite element method. J Sound Vib 333:6637–6650
23. Ehrhardt D, Harris R, Allen M (2014) Numerical and experimental determination of nonlinear normal modes of a circular perforated plate. In: De Clerck J (ed) Topics in modal analysis I, volume 7. Springer, Cham, pp 239–251
24. Peeters M, Kerschen G, Golinval JC (2011) Modal testing of nonlinear vibrating structures based on nonlinear normal modes: experimental demonstration. Mech Syst Signal Process 25:1227–1247
25. Zapico-Valle JL, García-Diéguez M, Alonso-Camblor R (2013) Nonlinear modal identification of a steel frame. Eng Struct 56:246–259
26. Ardeh HA, Allen MS (2013) Investigating cases of jump phenomena in a nonlinear oscillatory system. Presented at the 31st international modal analysis conference (IMAC XXXI), Garden Grove
27. Peeters M, Viguié R, Sérandour G, Kerschen G, Golinval JC (2009) Nonlinear normal modes, Part II: toward a practical computation using numerical continuation techniques. Mech Syst Signal Process 23:195–216
28. George TJ, Seidt J, Herman Shen MH, Nicholas T, Cross CJ (2004) Development of a novel vibration-based fatigue testing methodology. Int J Fatigue 26:477–486

UNCORRECTED PROOF

Author's Proof

AUTHOR QUERIES

AQ1. Please check if inserted page range for Ref. [9] is okay.
AQ2. Please check if inserted publisher location for Ref. [15] is okay.
AQ3. Please provide volume and page range for Ref. [18].

UNCORRECTED PROOF